



## OPEN Composite P3HT/ZnO thin films via FTM for improved charge transport in OFETs

A. S. M. Tripathi<sup>1,4</sup>✉, A. Dubey<sup>2</sup>, J. F. Blach<sup>3</sup>, F. Hochede<sup>3</sup>, S. Saitzek<sup>3</sup>, Y. Boussoualem<sup>1</sup> & A. Daoudi<sup>1</sup>

Zinc oxide (ZnO) nanorods, measuring 500 nm in diameter and 100 nm in length, were created in this article using an optimised hydrothermal low temperature technique. Using the newly created floating film transfer method, a large-scale oriented composite thin film of ZnO nanorod dispersion and poly (3-hexyl thiophene) is created. A thin film of the produced nanocomposite was placed to an active area of the p-type organic transistor in order to increase its mobility. The obtained high charge carrier hole mobility  $\mu$ , of  $>0.08 \text{ cm}^2/\text{Vs}$  along the orientation direction is caused by the nanocomposite thin film, as has been established. As per the prior research, the achieved result is approximately two orders higher and represents a more than four-fold boost over the pristine polymer device. The XRD and SEM were utilized to examine the crystalline characteristics of the nanostructure, and the atomic force microscope was employed to investigate the thin film morphology of the nanocomposite.

**Keywords** Floating film transfer method, Nanocomposite thin film, Field effect transistor, Nanorod

Over the past few years, solution-processable hybrid (organic/inorganic) semiconductors have attracted much interest due to their broad potential application in electronic devices<sup>1</sup>. Hybrid optoelectronics devices, like photovoltaic cells, organic light emitting diode, and Organic field effect transistors (OFETs), have been of great scientific interest in current research society<sup>2,3</sup>.

There are numerous OFET-based sensors in use today, including gas, light, chemical, pressure, and biological sensors<sup>4-10</sup>. Furthermore, OFETs can be fabricated on low-temperature solution processes and easily transferred on several substrates, including flexible substrates<sup>11</sup>. Hybrid materials are the main target to integrate the important properties of both types of materials. There are a lot of hybrid materials reported in photovoltaic and OLED applications<sup>12,13</sup>. Despite this development, OFETs are also fabricated based on this hybrid material. Moreover, there are more developments in this area by integrating the OFET for active matrix display, logic circuits, and memory chips<sup>14</sup>.

Hybrid materials have better electronic properties over the organic semiconductors and are lower compared to inorganic semiconductors<sup>15</sup>. On the other hand, materials with better electronic properties show high field-effect mobility. In order to manufacture low-cost transistors, regioregular polymers (P3HT) are willing more in organic electronics. For better device performance increasing the thin film crystalline properties and its interchain interactions are providing high mobility. Further electrical properties are enhanced by bringing in inorganic nanomaterials Zinc Oxide (ZnO) and Titanium oxide ( $\text{TiO}_2$ ) in the polymer matrix by controlling the free charge carriers<sup>16-20</sup>. Compared to amorphous silicon, ZnO possesses special qualities such a large band gap, transparency, and greater field effect mobility. ZnO nanoparticles are employed in electronic devices for electron extraction and as acceptors in hybrid materials<sup>21-27</sup>. To make the P3HT/ZnO-based OFETs, the dispersion of nanoparticles is still challenging in solution processing techniques. In this work, the composite thin films were fabricated using the recently developed Floating Film Transfer Method (FTM)<sup>28-30</sup>. This technique provides large area thin film with minimal wastage of material and high-in-charge carrier transport<sup>31-37</sup>. Thus we applied two approaches changing the material properties by blending the polymer with ZnO nanoparticles and controlling the thin-film morphology by FTM to enhance the OFET performance. Current state of art R.R. Navan et al. reported hybrid materials (P3HT/ZnO) for enhancing the OFET performance. According to the report, 25%, 40%, and 50% of ZnO's weight in P3HT are used for device fabrication<sup>38</sup>. According to his observation there is

<sup>1</sup>Unit of Dynamics and Structure of Molecular Materials (UDSMM), University of the Littoral Opal Coast, Dunkirk 4476, 59140, UR, France. <sup>2</sup>Rajiv Gandhi Institute of Petroleum Technology(RGIPT) Jais Amethi, Jais, U.P, India. <sup>3</sup>Solid State Catalysis and Chemistry Unit (UCCS), Centrale Lille, UMR 8181, University of Artois, CNRS, University of Lille, Lens 62300, France. <sup>4</sup>School of Electronics Engineering, VIT-AP University, Amaravati, A.P, India. ✉email: atul.tripathi@vitap.ac.in; atul.tripathi@univ-littoral.fr

enhancement in-charge carrier mobility from 25% to 40% and change at 50% of ZnO in P3HT. The result shows high mobility,  $\mu = 1.8 \times 10^{-3} \text{ cm}^2/\text{Vs}$  at 40% ZnO in P3HT and  $1.15 \times 10^{-3} \text{ cm}^2/\text{Vs}$  in pristine OFET<sup>38</sup>. M. Ba and co-authors also worked on a blend of P3HT: ZnO with concentrations of 50 mg/ml, 100 mg/ml, and 150 mg/ml in chlorobenzene solvent<sup>38,39</sup>. The results showing maximum charge transport  $\mu = 2.0 \times 10^{-3}$ ,  $7.5 \times 10^{-3}$ , and  $1.4 \times 10^{-3} \text{ cm}^2/\text{Vs}$ , while  $3 \times 10^{-4} \text{ cm}^2/\text{Vs}$  in pristine P3HT.

In this report, a polymer matrix was filled with ZnO nanorods that were synthesised in the lab in order to create a hybrid thin film for OFET applications. The aim of this experiment is to improve the charge carrier transport of solution-processed hybrid materials by varying the electrical properties of the P3HT solution through the blend of ZnO nanomaterials and quality control of the hybrid thin film using a recently developed new deposition technique. The hybrid film morphology characterized by atomic force microscopic (AFM) reveals the presence of anisotropic ZnO nanoparticles dispersed within a P3HT polymer film. Herein, FTM-prepared hybrid thin film (P3HT/ZnO) shows remarkable enhancement in p-type OFET mobility up to  $0.08 \text{ cm}^2/\text{Vs}$ , which is more than four times over the pristine polymer.

## Experimental method

ZnO nanorods were synthesized by a low-temperature hydrothermal process. Zinc acetate dihydrate ( $\text{Zn}(\text{OOCCH}_3)_2 \cdot 2\text{H}_2\text{O}$ , 98+%, Strem chemicals) and sodium hydroxide (NaOH,  $\geq 98\%$  Sigma Aldrich) were used as starting materials, and CetylTrimethylAmmonium Bromide (CTAB,  $\geq 99\%$ , Sigma Aldrich) was employed as surfactant. First, solution A is prepared by dissolving 0.025 mol of zinc acetate in 50 mL of distilled water. Then solution B is obtained by dissolving 0.001 mol of CTAB and 0.150 mol of NaOH. Solutions A and B were mixed and stirred vigorously for 1 h to obtain a clear solution. The resulting mixture was then transferred into an Equilabo stainless steel autoclave lined with Teflon and sealed tightly. For 20 h, hydrothermal treatments were conducted at 180 °C. The autoclave was then allowed to spontaneously cool to ambient temperature. Following opening, the white precipitate was collected by centrifugation and thrice washed with distilled water to get rid of any unreacted materials. Finally, the powder was dried at 90 °C in air. The growth mechanism of nanorods has already been described in the literature<sup>40–42</sup>. The  $\text{Zn}(\text{OH})_4^{2-}$  complex is formed when there is a large excess of hydroxide ions in the solution. A CTA + micelle and the Br-counterion are formed when the CTAB, an ionic solid, ionizes in an aqueous solution. With a lengthy hydrophobic tail and a tetrahedral head, the CTA + are positively charged. This cation allows the surfactant to function as an ionic carrier when it combines with  $\text{Zn}(\text{OH})_4^{2-}$  to generate a  $\text{CTA}^+ \cdot [\text{Zn}(\text{OH})_4]^{2-}$  complex through electrostatic interactions<sup>43</sup>. The growth units assemble along the polar faces and thus promote growth preferentially in the [0001] direction<sup>40</sup> ( $\vec{c}$  – axis). In conclusion, CTAB may be used as a capping agent to regulate ZnO nanostructure growth and morphology.

This experiment used conjugated polymer regioregular poly (3-hexyl thiophene) having regioregularity 95.2% and molecular weight (mW) 36,600 purchased from Oscilla (Sheffield, UK). Glycerol and ethylene glycol, which were obtained from Sigma Aldrich and VWR, were utilized as a hydrophilic viscous liquid substrate to create the polymer floating thin film binary combination. We purchased dehydrated chloroform from Sigma Aldrich and used it as a solvent to make the polymer solution.

A recently designed FTM has been employed to make the thin film. A P3HT/ZnO solution was made in  $\text{CHCl}_3$ , and 15  $\mu\text{l}$  hybrid solution was dropped into the middle of the aiding slider. Si/SiO<sub>2</sub> substrate with oxide thicknesses of up to 300 nm and capacitances of 10 nF/cm<sup>2</sup> were employed in the manufacturing of OFETs. Prior to undergoing the piranha treatment, the hydrophobic substrate was washed and then bathed in a mixture of 50–50% H<sub>2</sub>SO<sub>4</sub> and H<sub>2</sub>O<sub>2</sub>. The substrate treated with piranha was then dipped in OTS solution for 60 min, and washed following the previous manuscript. A source-drain electrode made of ~50 nm Au and ~5 nm Cr that had been thermally evaporated was employed. Additionally, the film that had undergone FTM processing was placed on the substrate and allowed to dry for 30 min at 50 °C.

We obtained the AFM image using the Veeco (Bruker) Multimode III and an optional C-AFM module. Two source meters (SMU B2901) were used to characterize the device's current-voltage (I-V). The driving gate voltage was applied via Channel 1, and the dielectric leakage current was measured. The drain current under ambient conditions was generated by using Channel 2 to supply the voltage between the source and drain.

## Result and discussion

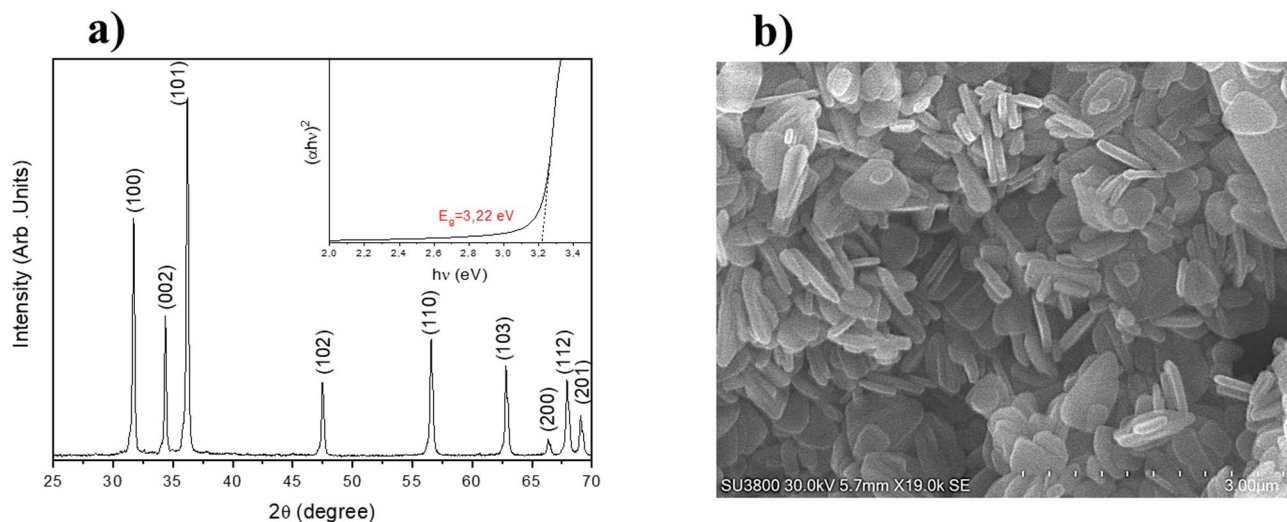
### ZnO characterization

Rigaku ULTIMA-IV diffractometer fitted with a Cu anticathode, Soller slits to control the divergence of X-ray beam, and a foil filter (nickel) to weaken the Cu K <sub>$\beta$</sub>  line, X-Ray diffraction (XRD) patterns were obtained. By utilizing the Bragg-Brentano setup, the registered angular range is 20°–70°, with a scanning rate of 0.15° per minute.

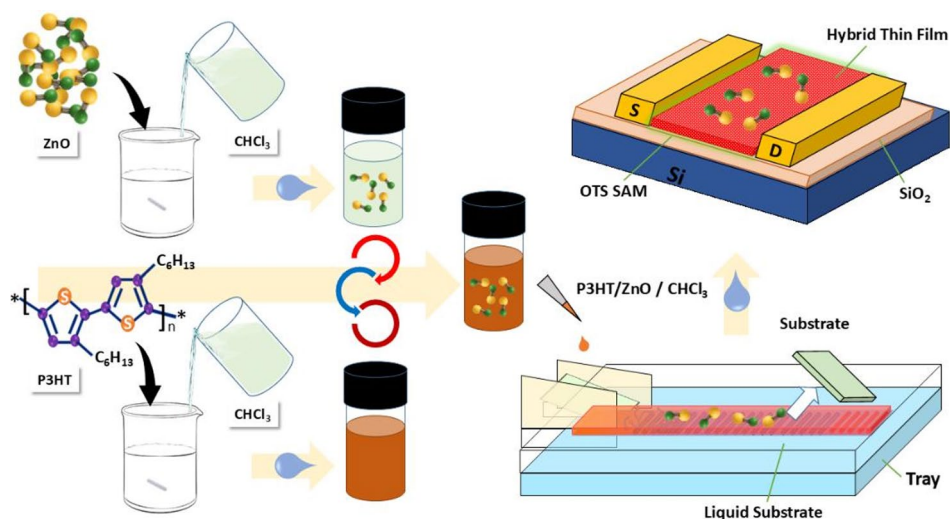
SEM images were recorded on a Hitachi SU3800 microscope using the Secondary Electron (SE) detector. The absorbance spectra obtained using an integrating sphere on a UV-2600 spectrophotometer (Shimadzu) were used to compute optical band gaps.

Figure 1(a) displays the XRD pattern obtained for ZnO nanorods. All observed reflections can be indexed to the hexagonal wurtzite structure (ICSD # 26170,  $a = 0.324986(1) \text{ nm}$ ,  $c = 0.520662(1) \text{ nm}$ )<sup>44</sup>, and no impurities were observed.

SEM micrographs in Fig. 1(b) present the morphology of ZnO powders where one observes the formation of rods whose average size is 500 and 100 nm for length and width, respectively. ZnO is n-type semiconductor with a direct bandgap<sup>45</sup>. We can determine this value using the absorbance spectrum and using the Tauc method by plotting  $(\text{ah}\nu)^2$  vs.  $h\nu$  (Inset Fig. 1a). The gap value is obtained by extrapolating the linear part of the curve with the intersection of the x-axis. This one was determined to be 3.22 eV and agrees with the literature<sup>46</sup>.



**Fig. 1.** (a) XRD pattern and Tauc plot (inset) of ZnO synthesized by hydrothermal method (b) SEM image showing the morphology of ZnO.



**Fig. 2.** Schematic process of composite thin film preparation for OFET device.

### Hybrid thin film and OFET fabrication

Figure 2 shows the step-wise process for the OFET fabrication. In the first stage, a hybrid solution ( $P_3HT/ZnO/CHCl_3$ ) was prepared in proportion to 10% ZnO. For this, separate solutions of 1%  $P_3HT/CHCl_3$  and 0.1%  $ZnO/CHCl_3$  w/w were mixed in 9:1. In the 2nd stage, a composite thin film is prepared by newly created single direction FTM technique. Film morphology optimization is followed by the previous casting parameter<sup>28</sup>. Previous work has provided further information about high-quality thin-film optimization and preparation<sup>29,30</sup>.

Without the need for a costly setup or an external force, this approach is comparable to the Langmuir-Blodgett method. It supplies the orientated thin film and then allows a natural process of self-assembly, unlike external forces. The direction of the film is reversed in this instance from the direction of spreading. The solvent's volatile nature leads to the formation of a floating solid film on the liquid substrate. This reliable film orientation process was based on solvent evaporation and the liquid substrate's opposing viscous force. On the liquid substrate, a floating solid film forms due to the solvent's volatile nature. The reliable mechanism of film orientation was based on the opposite viscous force of the liquid substrate and solvent evaporation. Film orientation can be easily seen by necked eyes using a polarizer sheet. The Fig. 2 shows the polymer film at a large scale up to  $\sim 21\text{ cm} \times 2\text{ cm}$  in length and width having thickness  $\sim 40$  to  $50\text{ nm}$ . The solid film was further transferred onto solid OFET chips between source and drain electrodes.

### Hybrid thin film morphology

A key factor in enhancing the device's performance is the thin film morphology. Atomic force microscopy (AFM) was used to precisely characterize the film's morphology and to analyze the distribution of the polymer and P3HT/ZnO using FTM methods, as shown in the complete analysis in Fig. 3 (a)–(d). As seen a featureless surface was found in the spin-coated film of pristine, However for FTM cast P3HT polymer film, nano-scale corrugations are aligned in the same direction across the surface as reported in previous manuscript<sup>47</sup>. The ZnO nanorods are evenly distributed throughout the polymer matrix. While FTM helps to align the polymer film, adding nanoparticles to the polymer also helps to create a more ordered structure. Similarly, Fig. 3 also indicates that there are no ZnO nanoparticle clusters present and that the P3HT/ZnO contacts in the layers have increased characteristics.

### Device electrical characterization

The electrical properties of devices made using the spin cast process and FTM are displayed in Fig. 4. All devices, with the exception of their current level, exhibit normal p-type behavior. The hybrid device displays a maximum current level of  $10^{-5}$ A, surpassing both the pristine polymer made using FTM and spin casting. Additional measurements of the same device's transfer properties were made at saturation conditions using the traditional standard equation.

$$I_D = \frac{1}{2} \mu_n C_{ox} \frac{W}{L} [V_{GS} - V_{th}]^2 \quad (1)$$

Where  $I_D$ ,  $\mu$ ,  $C_{ox}$ ,  $V_{GS}$ ,  $V_{th}$  stand for drain current, device mobility, oxide capacitance, gate voltage threshold voltage and  $W$ ,  $L$  are device dimension.

In pristine conditions,  $\mu = \sim 0.02 \text{ cm}^2/\text{Vs}$ , although the hybrid film exhibits high charge mobility,  $\mu > 0.08 \text{ cm}^2/\text{Vs}$ . In contrast to  $\mu = \sim 0.0021 \text{ cm}^2/\text{Vs}$ , in spin-cast, the FTM-coated pristine thin film exhibits a high charge carrier. These findings support the fact that the FTM-coated film enhanced the device's functionality. The device's performance is further improved by film preparation using ZnO nanorod through FTM.

Figure 4(b), (c) illustrates the transfer characteristics of OFET based on P3HT/ZnO film. The addition of ZnO to P3HT polymer increases drain current and mobility. The decrease in the density of traps in the P3HT/ZnO nanocomposites is linked to the notable improvement of charge mobility. A similar behavior were already observed by Xu et al.<sup>47</sup> for ZnO tetrapods or nanocrystals dispersed within the poly [2-methoxy,5-(2-ethylhexyloxy)-1,4-phenylenevinylene] polymer matrix. Also, we observed that the semiconducting P3HT

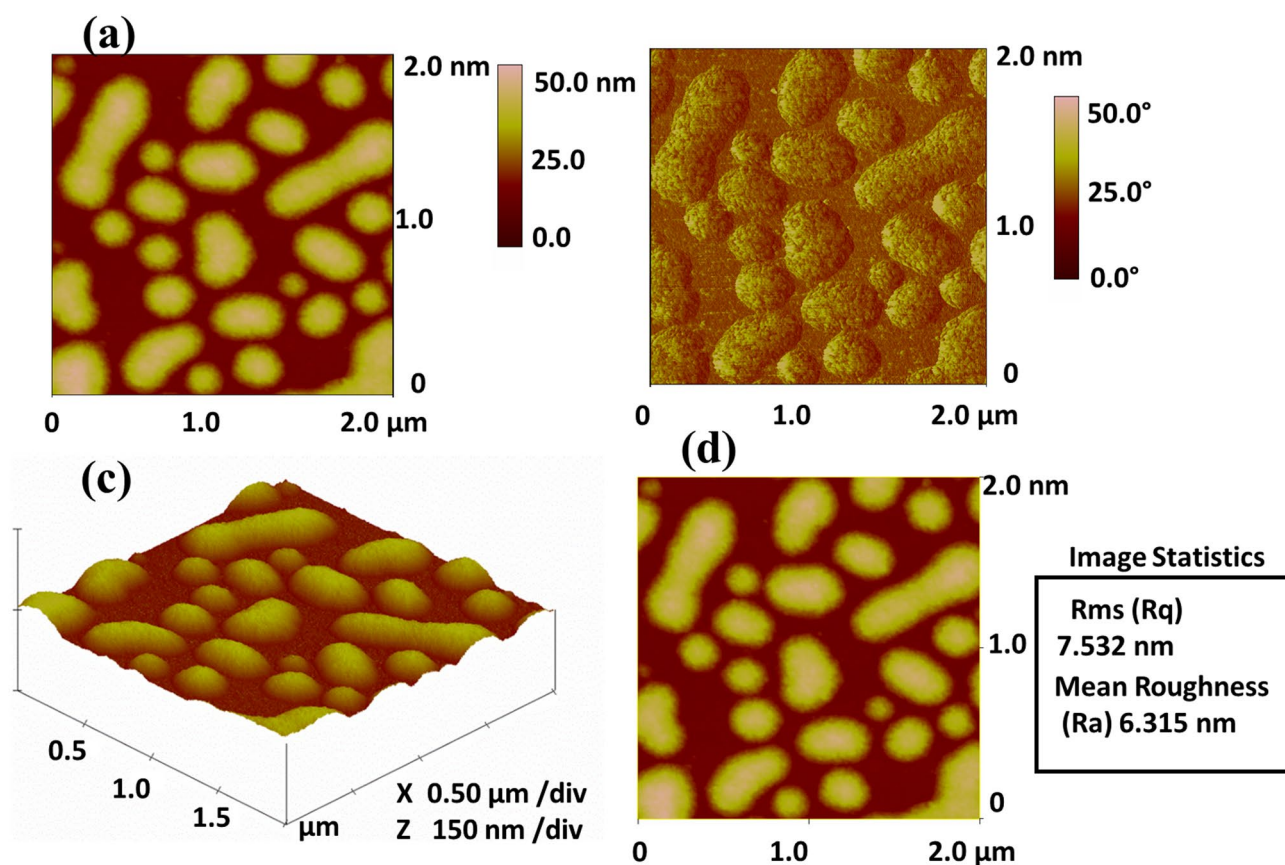


**Fig. 3.** Captured AFM images of P3HT/ZnO (a) height (b) phase (c) 3 D (d) Roughness analys.

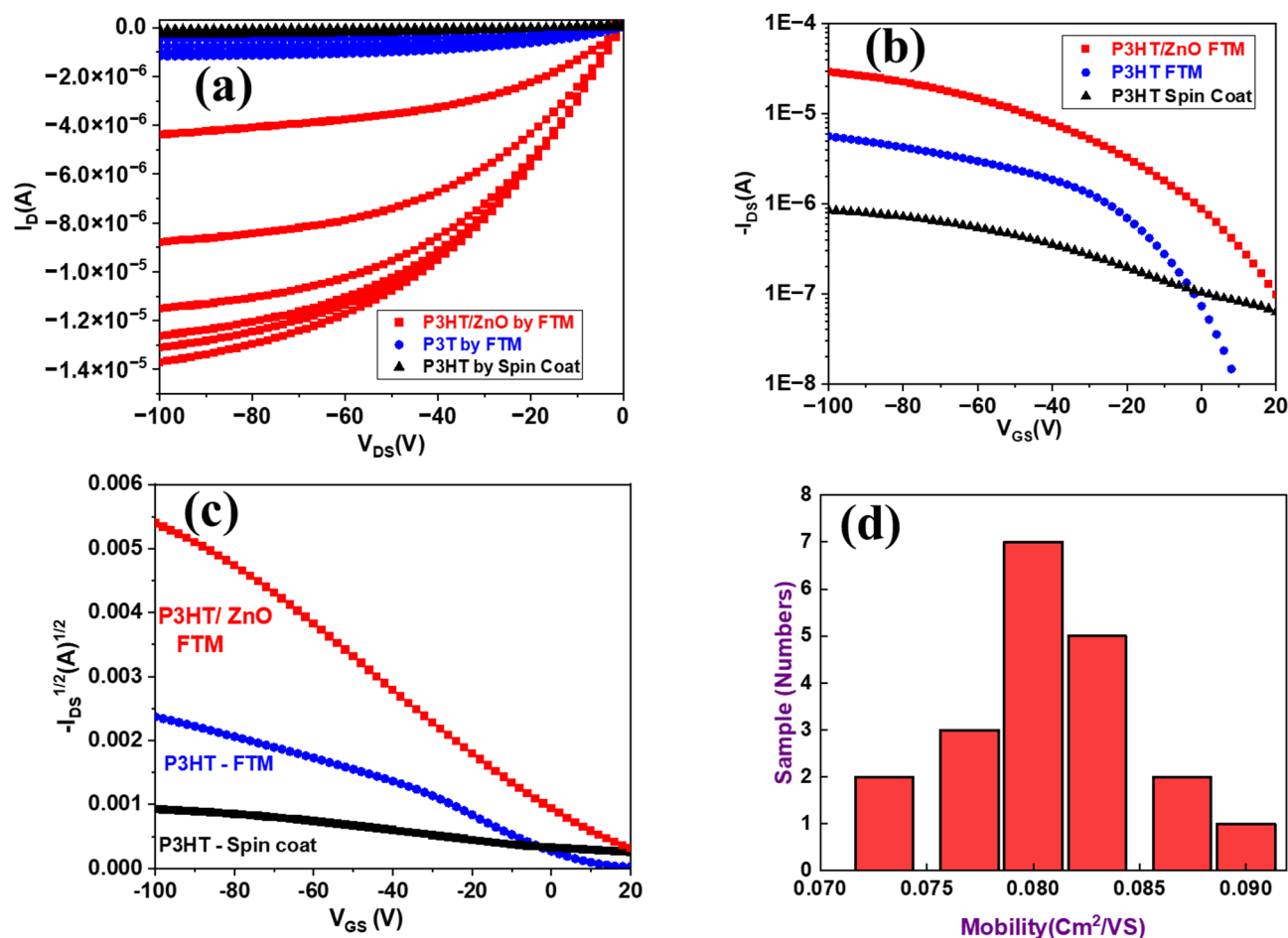


**Fig. 4.** Device output and transfer characteristics comparison and reproducibility (a) output (b) (c) transfer characteristics measured from 20 V to  $-100$  V (d) Reproducibility of device by preparing 20 device based on P3HT/ZnO by FTM.

Material	Mobility ( $\text{cm}^2/\text{Vs}$ )	Vth	$I_{\text{on}}/I_{\text{off}}$ Ratio	Stability	Refs.
P3HT/ZnO	$10^{-3}$ – $10^{-4}$	$-20$ to $-6$	150.9	-	49
P3HT/ZnO	$1.8 \times 10^{-3}$	-	-	-	38
P3HT/ZnO	$4 \times 10^{-3}$	$-0.76$	-	-	50
P3HT/ZnO	$10^{-3}$	15.6	44.5	-	39
P3HT/ZnO	$8 \times 10^{-2}$	$-2$ to $-4$	$10^4$	Ambient condition	This Work

**Table 1.** Comparison of previously reported P3HT/ZnO based OFET from this current work.

polymer retained its p-type behavior and shape following the incorporation of the ZnO nanorod. Thus, the drop in trap density and the self-reliant behavior of the (p-/n-type) can be concluded.

The transfer properties of the hybrid (P3HT/ZnO) and the pristine polymer (P3HT) are displayed in Fig. 4(b). When compared to pure P3HT made using FTM and spin coating, FTM-coated P3HT/ZnO exhibits higher current values. Table 1 shows reported device performance of P3HT/ZnO based hybrid materials and compare with the our work.

The repeatability of the device is displayed in Fig. 4(d) following the manufacture of 20 transistors. According to the graph, the average mobility is  $7 \times 10^{-2}$ , and the biggest and lowest peaks are at  $8 \times 10^{-2}$  and  $6 \times 10^{-2} \text{ cm}^2/\text{Vs}$ .

Figure 4(b), and (c), show the 10% ZnO in P3HT instances, at saturation condition, the hole mobility is detected in the nanocomposite OFETs.

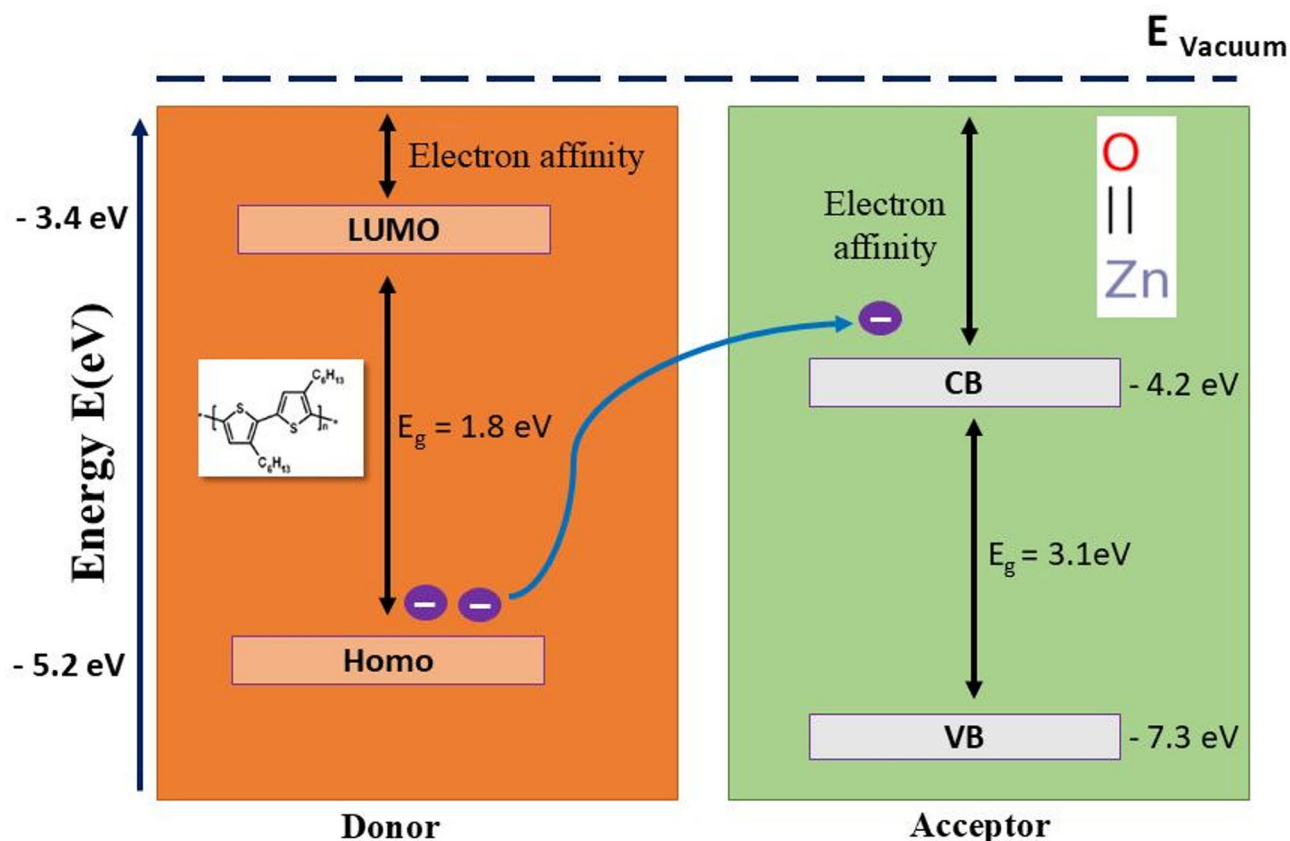


**Fig. 5.** Charge transfer mechanism in hybrid thin film.

Figure 5 shows the charge transporting operation in P3HT: ZnO film. The P3HT highest occupied molecular orbital (HOMO), the ZnO nanoparticle as the conduction band, and Au electrode fermi level expressed the operation of the devices.

In the device semiconducting layer induced the accumulation of holes at the interface at the condition  $V_{GS} < 0$ , which acts like a conductive p-type channel. Furthermore, the dispersion of nanoparticles in polymer upgrades the charge carrier passage and controls the traps that are available in the P3HT.

The key aspect of this manuscript is the reported remarkable enhancement in the hybrid device's performance achieved by tailoring ZnO nanoparticles with diameters of 500 nm and lengths of 100 nm. The solubility challenge of the nanorod is solved by a suitable option dispersion for integrating the hybrid material. The prepared polymer matrix was followed by the single direction FTM technique to control the thin film morphology. Whereas, the addition of this nanorod with polymer decreases the density trap and becomes a simple charge hopping. These two approaches enhance the device's mobility four times which is desired for OFET-based electronics devices.

## Conclusions

Finally, a report on the newly created, optimally synthesised Zinc Oxide (ZnO) Nano rod with a 500 diameter and 100 nm channel length was made. A poly (3-hexyl thiophene) large area composite thin film with a dispersed ZnO nanostructure was produced by employing the suggested single direction floating film transfer technique.

Moreover, the mobility of the p-type organic transistor is increased by the oriented nanocomposite thin film. This finding is striking since it is approximately two orders of magnitude higher in charge carrier mobility increment and four times higher ( $\mu > 0.08 \text{ cm}^2/\text{Vs}$ ) in pristine than previous study. The present findings have great potential to enhance large-scale composite thin-film mobility while minimising material waste.

## Data availability

The corresponding data will be provided on solicitation(atul.tripathi@vitap.ac.in).

Received: 27 August 2025; Accepted: 22 December 2025

Published online: 16 January 2026

## References

1. Sirringhaus, B. H. Device physics of solution-processed organic field-effect transistors. *Adv. Mater.* **17**, 2411–2425. <https://doi.org/10.1002/adma.200501152> (2005).

2. Kaloni, T. P., Giesbrecht, P. K., Schreckenbach, G. & Freund, M. S. Polythiophene: from fundamental perspectives to applications. *Chem. Mater.* **29**, 10248–10283. <https://doi.org/10.1021/acs.chemmater.7b03035> (2017).
3. Holliday, S. & Donaghey, J. E. Advances in charge carrier mobilities of semiconducting polymers used in organic transistors. *Chem. Mater.* **26**, 647–673. <https://doi.org/10.1021/cm402421p> (2014).
4. Someya, T., Sekitani, T., Iba, S., Kato, Y. & Kawaguchi, H. and T.Sakurai, A large-area, flexible pressure sensor matrix with organic field-effect transistors for artificial skin applications. **101** 9966–9970. (2024). <https://doi.org/10.1073/pnas.0401918101>
5. Park, B. et al. Evans, functional Self-Assembled monolayers for optimized photoinduced charge transfer in organic field effect transistors. *Adv. Mater.* **19**, 4353–4357. <https://doi.org/10.1002/adma.200602875> (2007).
6. Fukuda, H., Yamagishi, Y., Ise, M. & Takano, N. Gas sensing properties of poly-3-hexylthiophene thin film transistors. *Sens. Actuators B.* **108**, 414–417. <https://doi.org/10.1016/j.snb.2004.10.045> (2005).
7. Roberts, M. E., Mannsfeld, S., Queralto, N. & Bao, A. Z. Chemical and biological sensors based on organic thin-film transistors. *Am. Chem. Soc. Polym. Prepr. Div. Polym. Chem.* **384**, 343–353. <https://doi.org/10.1007/s00216-005-3390-2> (2008).
8. F.Yan, S. M., Mok, J. & Yu, H. L. W. Label-free DNA sensor based on organic thin film transistors. *Biosens. Bioelectron.* **24**, 1241–1245. <https://doi.org/10.1016/j.bios.2008.07.030> (2009).
9. P.Estrela, A. G., Stewart, F., Yan, P. & Migliorato Field effect detection of biomolecular interactions. *Electrochim. Acta.* **50**, 4995–5000. <https://doi.org/10.1016/j.electacta.2005.02.075> (2005).
10. Estrela, F. Y. P. & Migliorato, Y. M. P. H.Maeda,S.Inoue, polycrystalline silicon ion sensitive field effect transistors. *Appl. Phys. Lett.* **86**, 1–3. <https://doi.org/10.1063/1.1854192> (2005).
11. Sirringhaus, A. H., Kawase, T., Friend, R. H., Shimoda, T. & Inbasekaran, M. W.Wu, E.P.Woo. High-Resolution inkjet printing of All-Polymer transistor circuits. *Science* **290**, 2123–2126 (2000). <https://doi.org/www.jstor.org/stable/3081605>
12. Sanchez, C. & Julian, B. Applications of hybrid organic–inorganic nanocomposites. *J. Mater. Chem.* **15**, 3559–3592. <https://doi.org/10.1039/B509097K> (2005).
13. C.Melzer, E. J., Mihaleitchi, P. W. M. & Blom Hole transport in poly(phenylene vinylene)/methanofullerene bulk-heterojunction solar cells. *Adv. Funct. Mater.* **14**, 865–870. <https://doi.org/10.1002/adfm.200305156> (2004).
14. Barrett, C., Albert, J. D., Hidekazu, Y. & Joseph, J. An electrophoretic ink for all-printed reflective electronic displays. *Nature* **394**, 253–255. <https://doi.org/10.1038/28349> (1998).
15. Pandey, M. et al. Extreme orientational uniformity in large-area floating films of semiconducting polymers for their application in flexible electronics. *ACS Appl. Mater. Interfaces.* **13**, 38534–38543. <https://doi.org/10.1021/acsmi.1c09671> (2021).
16. Xie, T. et al. The mobility improvement of organic thin film transistors by introducing ZnO-nanrods as an active layer. *Sci. China Technological Sci.* **59**, 714–720. <https://doi.org/10.1007/s11431-016-6039-9> (2016).
17. Mok, S. M. & Chan, F. Y. H. L. W. Organic phototransistor based on poly(3-hexylthiophene)/ TiO<sub>2</sub> nanoparticle composite. *Appl. Phys. Lett.* **93**, 1–4. <https://doi.org/10.1063/1.2957981> (2008).
18. Hammer, M. S., Deibel, C. & Pflaum, J. Effect of doping of zinc oxide on the hole mobility of poly(3-hexylthiophene) in hybrid transistors. *Org. Electron.* **11**, 1569–1577. <https://doi.org/10.1016/j.orgel.2010.06.019> (2010).
19. Lüsse, B., Keum, C. M., Kasemann, D., Naab, B., Leo, K. & Z.Bao and Doped organic transistors. *Chem. Rev.* **116**, 13714–13751. <https://doi.org/10.1021/acs.chemrev.6b00329> (2016).
20. Tsoulos, G. V., Beach, M. A. & Swales, S. C. Performance enhancement of p-type organic thin film transistors using zinc oxide nanostructures. *Int. J. Nanosci.* **10**, 761–764. <https://doi.org/10.1142/S0219581X11008800> (2011).
21. Masuda, S., Okumura, K. K. Y. & Tabata, S. M. H. Transparent thin film transistors using ZnO as an active channel layer and their electrical properties. *J. Appl. Phys.* **93**, 1624–1630. <https://doi.org/10.1063/1.1534627> (2003).
22. Carcia, P. F., McLean, R. S. & Reilly, M. H. Transparent ZnO thin-film transistor fabricated by Rf Magnetron sputtering. *Appl. Phys. Lett.* **82**, 1117–1119. <https://doi.org/10.1063/1.1553997> (2003).
23. Hoffman, R. L., Norris, B. J. & Wager, J. F. ZnO-based transparent thin-film transistors. *Appl. Phys. Lett.* **82**, 733–735. <https://doi.org/10.1063/1.1542677> (2003).
24. Nishii, J. et al. High mobility thin film transistors with transparent ZnO Channels, *Jpn. J. Appl. Phys.* **42**, L347–349. <https://doi.org/10.1143/JJAP.42.L347> (2003).
25. Carcia, P. F. et al. A comparison of zinc oxide thin-film transistors on silicon oxide and silicon nitride gate dielectrics. *J. Appl. Phys.* **102**, 074512. <https://doi.org/10.1063/1.2786869> (2007).
26. Fortunato, E. M. C., Barquinha, P. M. C., A.C.M.B.G.Pimentel, M. F. & Gonçalves, R. F. P. L.M.N.Pereira, Wide-bandgap high-mobility ZnO thin-film transistors produced at room temperature. *Appl. Phys. Lett.* **85**, 2541–2543. <https://doi.org/10.1063/1.1790587> (2004).
27. K.Remashan, J. H., Jang, D. K., Hwang, S. J. & Park ZnO-based thin film transistors having high refractive index silicon nitride gate. *Appl. Phys. Lett.* **91**, 182101. <https://doi.org/10.1063/1.2804566> (2007).
28. Tripathi, A. S. M., Pandey, M., Nagamatsu, S., Pandey, S. S. & Hayase, S. Casting control of Floating-films into Ribbon-shape structure by modified dynamic FTM. *J. Phys. Conf. Ser.* **924**, 012014. <https://doi.org/10.1088/1742-6596/924/1/012014> (2017).
29. Tripathi, A. S. M., Pandey, M., Sadakata, S. & Takashima, S. N. W. Anisotropic charge transport in highly oriented films of semiconducting polymer prepared by ribbon-shaped floating film. *Appl. Phys. Lett.* **112**, 2–4. <https://doi.org/10.1063/1.5000566> (2018).
30. Tripathi, A. S. M. et al. Implication of molecular weight on optical and charge transport anisotropy in PQT-C12 films fabricated by dynamic FTM. *ACS Appl. Mater. Interfaces.* **11**, 28088–28095. <https://doi.org/10.1021/acsmi.9b06568> (2019).
31. Tripathi, A. S. M., Gupta, R. K., Sharma, S. & Nagamatsu, S. .Pandey, molecular orientation and anisotropic charge transport in the large area thin films of regioregular Poly(3-alkylthiophenes) fabricated by ribbon-shaped FTM. *Org. Electron.* **81**, 105687. <https://doi.org/10.1016/j.orgel.2020.10.043> (2020).
32. Tripathi, A. S. M., Kumari, N., Nagamatsu, S. & Hayase, S. .Pandey, facile fabrication of large area oriented conjugated polymer films by ribbon-shaped FTM and its implication on anisotropic charge transport. *Org. Electron.* **65**, 1–7. <https://doi.org/10.1016/j.orgel.2018.10.043> (2019).
33. Pandey, R. K., Tripathi, A. S. M., Pandey, S. S. & Prakash, R. Optoelectrical anisotropy in graphene oxide supported polythiophene thin films fabricated by floating film transfer. *Carbon* **147**, 252–261. <https://doi.org/10.1016/j.carbon.2019.02.086> (2019).
34. Tripathi, A. S. M. et al. Orientation in large-area semiconducting 2-amino-anthracene thin films fabricated by dynamic floating film transfer method. *Thin Solid Films.* **742**, 139044. <https://doi.org/10.1016/j.tsf.2021.139044> (2022).
35. Kumari, N., Tripathi, A. S. M., Sadakata, S., Pandey, M. & Nagamatsu, S. Hayase, 2D positional profiling of orientation and thickness uniformity in the semiconducting polymers thin films. *Org. Electron.* **68**, 221–229. <https://doi.org/10.1016/j.orgel.2019.02.011> (2019).
36. Pandey, M. et al. Unidirectionally aligned donor–acceptor semiconducting polymers in floating films for high-performance unipolar n-channel organic transistors. *Adv. Electron. Mater.* **9**, 2201043. <https://doi.org/10.1002/aem.202201043> (2023).
37. Sharma, S. et al. High field-effect mobility in oriented thin films of D-A type semiconducting polymers by engineering stable interfacial system. *Chem. Eng. J.* **469**, 143932. <https://doi.org/10.1016/j.cej.2023.143932> (2023).
38. Navan, R. R., Bharati, P., Baghini, M. S. & Bahadur, D. V.R.Rao, mobility enhancement of solution-processed Poly(3-Hexylthiophene) based organic transistor using zinc oxide nanostructures. *Compos. Part. B: Eng.* **43**, 1645–1648. <https://doi.org/10.1016/j.compositesb.2011.08.007> (2012).
39. Ba, M. et al. Controlling of hysteresis by varying ZnO-Nanoparticles amount in P3HT:ZnO hybrid Thin-Film transistor: modeling. *J. Electron. Mater.* **52**, 1203–1215. <https://doi.org/10.1007/s11664-022-10066-2> (2023).

40. Sun, X. M., Deng, X. C. Z. X. & Li, Y. D. A CTAB-assisted hydrothermal orientation growth of ZnO nanorods. *Mater. Chem. Phys.* **78**, 99–104. [https://doi.org/10.1016/S0254-0584\(02\)00310-3](https://doi.org/10.1016/S0254-0584(02)00310-3) (2003).
41. Unirii, S. Hydrothermal growth of ZnO nanowires. *Sci. Bull. Valahia university- Mater. Mech.* **7**, 9–13 (2012). [https://fsim.valahia.ro/sbmm.html/docs/2012/materials/2\\_Chitanu\\_2012.pdf](https://fsim.valahia.ro/sbmm.html/docs/2012/materials/2_Chitanu_2012.pdf)
42. Maiti, U. N., Nandy, S., Karan, S. & Mallik, B. .Chattopdhyay, enhanced optical and field emission properties of CTAB-assisted hydrothermal grown ZnO nanorods. *Appl. Surf. Sci.* **254**, 7266–7271. <https://doi.org/10.1016/j.apsusc.2008.05.311> (2008).
43. Bricha, M., Belmamouni, Y., Essassi, E. M., Ferreira, J. M. F. & Khalil, E. I. Surfactant-assisted hydrothermal synthesis of hydroxyapatite nanopowders. *J. Nanosci. Nanotechnol.* **12**, 8042–8049. <https://doi.org/10.1166/jnn.2012.6664> (2012).
44. Abrahams, S. C. & Bernstein, J. L. Remeasurement of the structure of hexagonal ZnO. *Acta Crystallogr. Sect. B Struct. Crystallogr. Cryst. Chem.* **25**, 1233–1236. <https://doi.org/10.1107/s0567740869003876> (1969).
45. Janotti, A., Walle, C. G. & Van De, C. G. Fundamentals of zinc oxide as a semiconductor. *Rep. Prog Phys.* **72**, 126501. <https://doi.org/10.1088/0034-4885/72/12/126501> (2009).
46. V.Srikant, D. R. & Clarke On the optical band gap of zinc oxide. *J. Appl. Phys.* **83**, 5447–5451. <https://doi.org/10.1063/1.367375> (1998).
47. Tripathi, A. S. M., Boussoualem, Y. & Daudi, A. Large area polymer thin film towards high-sensitivity BGBC-OFET based phototransistor. *Opt. Mater.* **146**, 114614. <https://doi.org/10.1016/j.optmat.2023.114614> (2023).
48. Xu, Z. X. et al. Nanocomposite field effect transistors based on zinc oxide/polymer blends. *Appl. Phys. Lett.* **90**, 1–4. <https://doi.org/10.1063/1.2740478> (2007).
49. Kumar, A. et al. Performance enhancement of p-type organic thin-film transistors using zinc oxide nanostructures. *Int. J. Nanosci.* **10**, 761–764. <https://doi.org/10.1142/S0219581X11008800> (2011).
50. Xie, T. et al. The mobility improvement of organic thin-film transistors by introducing ZnO nanorods as an active layer. *Sci. China Technol. Sci.* **59**, 714–720. <https://doi.org/10.1007/s11431-016-6039-9> (2016).

## Acknowledgements

The authors thank ULCO, Region Hauts-de-France, for financial support for this project.

## Author contributions

Dr. Atul Shankar Mani Tripathi: Conceptualization, Methodology, Writing– original draft, editing. Dr. A. Dubey : Writing– review and discussion. Dr. J. F Blach : ZnO Synthesis, Writing– review. Mr. F. Hochede : ZnO Synthesis. Dr. S. Saitzek: ZnO Synthesis. Dr. Y. Boussouale : Supervision, Writing– review. Dr. A Daoudi : Supervision, Writing– review.

## Funding

The authors would like to express their gratitude for financial assistance in the publication Provided by VIT-AP University, Amaravati, Andhra Pradesh, India.

## Declarations

## Competing interests

The authors declare no competing interests.

## Additional information

**Correspondence** and requests for materials should be addressed to A.S.M.T.

**Reprints and permissions information** is available at [www.nature.com/reprints](http://www.nature.com/reprints).

**Publisher's note** Springer Nature remains neutral with regard to jurisdictional claims in published maps and institutional affiliations.

**Open Access** This article is licensed under a Creative Commons Attribution-NonCommercial-NoDerivatives 4.0 International License, which permits any non-commercial use, sharing, distribution and reproduction in any medium or format, as long as you give appropriate credit to the original author(s) and the source, provide a link to the Creative Commons licence, and indicate if you modified the licensed material. You do not have permission under this licence to share adapted material derived from this article or parts of it. The images or other third party material in this article are included in the article's Creative Commons licence, unless indicated otherwise in a credit line to the material. If material is not included in the article's Creative Commons licence and your intended use is not permitted by statutory regulation or exceeds the permitted use, you will need to obtain permission directly from the copyright holder. To view a copy of this licence, visit <http://creativecommons.org/licenses/by-nc-nd/4.0/>.

© The Author(s) 2026